DYNAMIC RESPONSE OF A BURIED PIPE IN A SEISMIC ENVIRONMENT

by

S.K. Datta, A.H. Shah and N. El-Akily

CUMER-80-5 August 1980

DYNAMIC BEHAVIOR OF A BURIED PIPE IN A SEISMIC ENVIRONMENT

S.K. Datta, Professor
Department of Mechanical Engineering
University of Colorado, Boulder
Member, ASME

A.H. Shah, Associate Professor
Department of Civil Engineering
University of Manitoba, Winnipeg

N. El-Akily, Assistant Professor
Department of Mechanical Engineering
University of Colorado, Boulder

Abstract

Axisymmetric dynamic response of a buried pipe due to an incident compressional wave is the subject of this investigation. The pipe has been modelled as a thin cylindrical shell of linear homogeneous isotropic elastic material embedded in a linear isotropic homogeneous elastic medium of infinite extent. The response characteristics of the pipe due to changes in the material properties of the surrounding medium have been carefully studied. It is found that even at long wavelengths and low frequencies the dynamic response is significantly altered by the changes in the Poisson's ratio and the rigidity modulus of the surrounding medium. Further it is found that there are real resonant frequencies of the pipe which are also significantly dependent on these quantities as well as on the wavelength.

1. Introduction

Dynamic response of buried pipelines to seismic excitation has been a subject of considerable interest in recent years. The interest in the subject originates from the desire to design lifelines like gas and water/sewer pipelines against severe damage from earthquakes. The damage to buried pipelines is caused by landslides, liquefaction of soil, faulting and also due to shaking by traveling seismic waves.

Several investigators have recently studied the dynamic response of underground pipelines to seismic excitation. References to these works can be found in the review articles [1, 2, 3, 4]. Most of these works have treated the pipeline as a continuous or segmented beam and have not taken into account the dynamic interaction between the pipe and its surrounding medium.

The departure from the beam model is in the works of Ariman, et al. [2, 5] and in those of Novak and his co-workers [6, 7, 8], where the authors have considered the shell model of the pipe. However, the interaction of the pipe and the soil has not been considered.

In our recent studies [9, 10, 11] it has been shown that the interaction between the pipe and its environment significantly influences the displacements of the pipe wall and the stresses arising in it. It has also been found [9, 10] that the depth of the embedment of the pipe also affects the pipe response.

In this paper we have examined in detail the interaction effects on the dynamic response. In an earlier paper [11] we presented a quasi-static analysis of the problem in which the inertia effects were neglected. It was shown that except for very long wavelengths the pipe does not in general follow the motion of the ground. This implies that the inertia effects should have considerable influence on the response of the pipe. Thus the object of this paper is to analyze the full dynamic problem.

The related problems of the free and forced vibrations of a pipe in an acoustic medium have received considerable attention in the past [12, 13]. The vibration of a pipe in an elastic medium is complicated by the coupling of the longitudinal and shear waves generated in the surrounding medium. As in the case of a freely vibrating pipe in an acoustic medium it is found that there may exist resonant frequencies for a pipe freely vibrating in an elastic medium. However, in the latter case the existence of the resonant frequencies depends on the rigidity ratio of the pipe and its surrounding elastic medium.

We have also considered the forced vibration of the pipe due to an incident longitudinal wave. It is shown that the displacement of the pipe wall and the axial stress in it depend critically on the Poisson's ratio and the rigidity modulus of the surrounding medium.

2. Equations and Solution

As shown in [11] the equations governing the axisymmetric motion of a shell element are given by

$$[- \frac{1}{R^2} (E_p + D/R^2) + k_x^2 Gh \frac{\partial^2}{\partial x^2} - \rho_s h \frac{\partial^2}{\partial t^2}] w + k_x^2 Gh \frac{\partial \Psi_x}{\partial x} - \frac{E_p \nu}{R} \frac{\partial u}{\partial x} + p_1^* = 0 \qquad (1)$$

$$- k_x^2 Gh \frac{\partial w}{\partial x} + [D \frac{\partial^2}{\partial x^2} - k_x^2 Gh - \rho_x I \frac{\partial^2}{\partial t^2}] \Psi_x + [\frac{D}{R} \frac{\partial^2}{\partial x^2} - \frac{\rho_s I}{R} \frac{\partial^2}{\partial t^2}] u + p_2^* = 0 \qquad (2)$$

$$\frac{E_p \nu}{R} \frac{\partial w}{\partial x} + [\frac{D}{R} \frac{\partial^2}{\partial x^2} - \frac{\rho_s I}{R} \frac{\partial^2}{\partial t^2}] \Psi_x + [E_p \frac{\partial^2}{\partial x^2} - \rho_s h \frac{\partial^2}{\partial t^2}] u + p_3^* = 0 \qquad (3)$$

Here u, w are the axial and radial displacements of a point on the shell-middle surface (see Figure 1) and Ψ_x is the rotation of the normal to this surface in the meridianal plane. The other shell parameters appearing above are defined as follows.

$R \equiv$ Mean Radius

$h \equiv$ Thickness

$E_p = \frac{Eh}{1 - \nu^2}$, $E \equiv$ Young's Modulus, $\nu \equiv$ Poisson's Ratio

$D = \frac{E_p h^2}{12}$

$G \equiv$ Shear Modulus

$\rho_s \equiv$ Density

$I = \frac{h^3}{12}$

$k_x \equiv$ Shear correction factor, taken as $\frac{\pi}{\sqrt{12}}$

The vector $\underset{\sim}{p}^*$ represents the force and moment exerted per unit area by the surrounding medium on the shell and has the components

$$p_1^* = (1 + \frac{h}{2R})\,\tau_{rr}^* \quad , \quad p_2^* = \frac{h}{2}\,p_3^* \quad , \quad p_3^* = (1 + \frac{h}{2R})\,\tau_{rx}^* \tag{4}$$

The stress components τ_{rr}^* and τ_{rx}^* arise from the motion of the surrounding medium and are evaluated at $r = R + \frac{h}{2}$.

The displacement $\underset{\sim}{u}(r, \theta, x, t)$ of a point of the outer medium satisfies the equations of motion

$$\tau^2 \underset{\sim}{\nabla}\underset{\sim}{\nabla} \cdot \underset{\sim}{u} - \underset{\sim}{\nabla} \wedge \underset{\sim}{\nabla} \wedge \underset{\sim}{u} = \frac{1}{c_2^2}\,\frac{\partial^2 \underset{\sim}{u}}{\partial t^2} \tag{5}$$

where

$$\tau = \sqrt{\frac{2(1-\sigma)}{1-2\sigma}} \quad , \qquad c_2 = \sqrt{\frac{\mu}{\rho}}$$

σ is the Poisson's ratio and c_2 is the shear wave speed.

Since the object of the present investigation is to analyze the motion of the shell excited by an incoming traveling seismic wave, it will be assumed that $\underset{\sim}{u}$ is composed of two parts. The part due to the incident disturbance will be denoted by $\underset{\sim}{u}^{(i)}$, whose components may be represented for axisymmetric motion as

$$\begin{aligned} u_r^{(i)} &= - u_o R\sqrt{\xi^2 - k_1^2}\;\; I_1 (\sqrt{\xi^2 - k_1^2}\, r) \cos \xi\,(x - ct) \\ u_x^{(i)} &= u_o \,\xi R\, I_o (\sqrt{\xi^2 - k_1^2}\; r) \sin \xi\,(x - ct) \end{aligned} \tag{6}$$

where I_n is the modified Bessel function of the first kind. In writing (6) it has been assumed that the disturbance is in the form of a longitudinal wave. Clearly $\underset{\sim}{u}^{(i)}$ given by (6) with $k_1 = \omega/c_1 = c\xi/c_1$ satisfies (5) and is a traveling wave of wavelength $\lambda = 2\pi/\xi$, moving with speed c along the axis of the pipe. For the special case of a plane longitudinal wave moving along the axis of the pipe (6) will reduce to

$$u_r^{(i)} = 0 \quad , \quad u_x^{(i)} = u_o \xi R \sin \xi (x - c_1 t) \tag{7}$$

The other part of $\underset{\sim}{u}$, denoted by $\underset{\sim}{u}^{(s)}$, may then be written as (see [11]),

$$\begin{aligned} u_r^{(s)} &= -[A \frac{\gamma}{R} K_1 (\gamma \frac{r}{R}) + B\xi K_1 (\delta \frac{r}{R})] \cos \xi (x - ct) \\ u_x^{(s)} &= [A\xi K_o (\gamma \frac{r}{R}) + B \frac{\delta}{R} K_o (\delta \frac{r}{R})] \sin \xi (x - ct) \end{aligned} \tag{8}$$

Here K_n is the modified Bessel function of the second kind and

$$\gamma = \sqrt{\ell^2 - \epsilon^2} \quad , \quad \delta = \sqrt{\ell^2 - \tau^2 \epsilon^2} \quad , \quad \epsilon = \omega R/c_1 \quad , \quad \ell = \xi R \tag{9}$$

The constants A and B are chosen so that the displacement is continuous at the shell outer surface, i.e.,

$$u_r^{(s)} = w - u_r^{(i)} , \quad u_x^{(s)} = u + \frac{h}{2} \Psi_x - u_x^{(i)} \tag{10}$$

Once $u_r^{(s)}$, $u_x^{(s)}$ are known, they can be used to calculate the stresses $\tau_{rr}^{(s)*}$, $\tau_{rx}^{(s)*}$ arising from them at $r = R + h/2$. Assuming that

$$w = \bar{w} \cos \xi (x - ct) \quad , \quad \Psi_x = \bar{\Psi}_x \sin \xi (x - ct) \quad , \quad u = \bar{u} \sin \xi (x - ct) \tag{11}$$

it was shown in [11] that

$$p_1^* = \frac{\mu}{R}[\,T_{11} w_o + \frac{h}{2} T_{12} \bar{\Psi}_x + T_{13} u_o\,] \cos \xi\,(x - ct) + (1 + \frac{m}{2})\, \tau_{rr}^{(i)*}$$

$$p_3^* = \frac{\mu}{R}[\,T_{13} w_o + \frac{h}{2} T_{23} \bar{\Psi}_x + T_{33} u_o\,] \sin \xi\,(x - ct) + (1 + \frac{m}{2})\, \tau_{rx}^{(i)*} \tag{12}$$

$$p_2^* = \frac{h}{2}\, p_3^*$$

where the elements T_{ij} of the matrix T are given by

$$T_{11} = -(1 + m/2)\,[\,\delta\, \frac{\tau^2 \epsilon^2 K_o(\mathcal{B})\, K_o(\mathcal{A})}{\mathcal{D}} + \frac{2}{1 + m/2}\,]$$

$$T_{12} = T_{21} = T_{13} = T_{31} = -\ell\,(1 + m/2)\,[\,2 - \frac{\tau^2 \epsilon^2 K_1(\mathcal{B})\, K_o(\mathcal{A})}{\mathcal{D}}\,] \tag{13}$$

$$T_{22} = T_{33} = T_{23} = T_{32} = -\frac{(1 + m/2)\,\tau^2 \epsilon^2 \gamma\, K_1(\mathcal{A})\, K_1(\mathcal{B})}{\mathcal{D}}$$

$$\mathcal{D} = \ell^2 K_o(\mathcal{A})\, K_1(\mathcal{B}) - \gamma\delta\, K_1(\mathcal{A})\, K_o(\mathcal{B})$$

and

$$m = h/R\,, \quad w_o = \bar{w} + u_o \gamma\, I_1(\mathcal{A})\,, \quad u_o = \bar{u} - u_o \ell\, I_o(\mathcal{A})$$

$$\mathcal{A} = (1 + m/2)\,\gamma\,, \quad \mathcal{B} = (1 + m/2)\,\delta$$

Finally equations for the determination of $\bar{w}$, $\bar{\Psi}_x$ and $\bar{u}$ are obtained by substituting (11) and (12) in (1) - (3). In matrix notation these can be written as

$$[\,A - MT - \Omega^2 B\,]\,U = -MT\,U^{(i)} + MT^{(i)} \tag{14}$$

Here A and B are symmetrix 3×3 matrices having the elements

$$
\begin{aligned}
A_{11} &= 2Nm\,(1 + m^2/12) + k_x^2\, m\ell^2 \;, \qquad B_{11} = 1 \\
A_{12} &= -\,2k_x^2\,\ell \;, \qquad B_{12} = 0 \\
A_{13} &= 2N\nu\,\ell m \;, \qquad B_{13} = 0 \\
A_{22} &= \frac{4}{m}\left(\frac{N}{6}\, m^2\ell^2 + k_x^2\right) , \qquad B_{22} = \frac{1}{3} \\
A_{23} &= \frac{1}{3}\, Nm^2\ell^2 \;, \qquad B_{22} = \frac{m}{6} \\
A_{33} &= 2Nm\ell^2 \;, \qquad B_{33} = 1
\end{aligned}
\tag{15}
$$

Also,

$$
M = \mu/G \;, \qquad N = \frac{1}{1 - \nu} \;, \qquad U_1^{(i)} = -\gamma\, I_1\,(\mathcal{A})
$$

$$
U_2^{(i)} = 0 \;, \qquad U_3^{(i)} = \ell\, I_o\,(\mathcal{A})
$$

$$
T_1^{(i)} = (\tau^2\epsilon^2 - 2\ell^2)\, I_o\,(\mathcal{A}) + \frac{2\gamma}{1 + m/2}\, I_1\,(\mathcal{A})
$$

$$
T_2^{(i)} = T_3^{(i)} = 2\gamma\ell\, I_1\,(\mathcal{A})
$$

$$
U_1 = \bar{w}/u_o \;, \qquad U_2 = \frac{h}{2}\,\bar{\Psi}_x/u_o \;, \qquad U_3 = \bar{u}/u_o
$$

$$
\Omega^2 = \frac{\rho_s\, hR}{G}\,\omega^2 = \tau^2\epsilon^2\, Mm\left(\frac{\rho_s}{\rho}\right)
$$

It should be pointed out here that Eq. (14) represents the equation for the determination of the displacement of, and the rotation normal to, the middle surface when the pipe is excited by an axially propagating longitudinal wave. The excitation is given by the right hand side of Eq. (14). Clearly the matrix T is independent of the nature of the excitation and depends solely on the geometry of the pipe, the material properties of the surrounding medium and, of course, on the wavelength and wave-speed of the excitation. So for a different excitation only $U^{(i)}$ and $T^{(i)}$ will be changed. Further, the equation determining the frequency of free vibration of the pipe in an elastic medium is given by

$$\det [A - MT - \Omega^2] = 0 \tag{16}$$

In general these frequencies are complex and depend on M as well as on other material and geometrical parameters of the shell and its surrounding medium. The real frequencies can exist only if

$$\varepsilon < \ell/\tau \tag{17}$$

These are discussed in the following section. Note that (17) implies that $c < c_2$.

3. Numerical Results and Discussion

Eq. (16) was solved for real frequencies for different values of M and the Poisson's ratio, σ, of the outer medium. These are shown in Tables 1 and 2. The following parameters were chosen for the shell.

$$h/R = .05 , \quad \nu = 0.3 , \quad \rho_s/\rho = 2.9266$$

It was found that there were no real frequencies for small M and for M between 0.1 and 1 there is only one real frequency, which lies between the frequencies of the first and second flexural modes of free vibration of the pipe in vacuum. It is further noted that if $\ell \leq \frac{\pi}{3}$ then there are no real frequencies for any value of M. This is to be contrasted with the case of a shell vibrating in an acoustic medium in which case it was found [12] that there was always one real frequency for all ℓ. Also, the real frequency exists for smaller values of ℓ as M increases. For example, when M = 0.1 the real frequency occurs first for $\ell = 5\pi/3$ whereas, when M = 0.3 it occurs first for $\ell = 5\pi/6$ and when M = 1 it is for $\ell = 2\pi/3$. It is observed that the frequency of free vibration decreases with the increase in the rigidity ratio of the soil and the pipe. Increasing the Poisson's ratio also decreases the frequency.

As an example of forced vibration Eq. (14) was then solved for U for different ℓ, ϵ, M and σ with the same shell parameters indicated above. Knowing U the axial stress N_{xx} is then calculated from the equation

$$N_{xx} = \frac{E_p u_o}{R} \left[\ell U_3 + \nu U_1 + \frac{1}{6} m\ell \, U_2 \right] \tag{18}$$

In order to exemplify the dynamic effect $|w/w^{static}|$ ($\equiv$ W) and $|N_{xx}/N_{xx}^{static}|$ ($\equiv$ N) have been plotted in Figures 2 - 13 against ϵ for different ℓ and M. Here w^{static} and N_{xx}^{static} are obtained by solving Eq. (14) when $\epsilon = 0$.

These static solutions are discussed in [11].

Figures 2 - 5 show the variations of W and N with ϵ and M for $\ell = \pi/6$ and $\sigma = 0.25$ and 0.45, respectively. It is seen from Fig. 2 that for small M, W increases slightly from 1.0 for small ϵ, then decreases to a minimum at about $\epsilon = 0.4$ and continually increases with ϵ thereafter. Both figures 2 and 3 show that for all M, W drops below 1.0 for small ϵ, goes through minima and then increases with ϵ. Comparing Figs. 2 and 3 it is observed that changing the Poisson's ratio has pronounced effect on the dynamic response of the shell. This is to be contrasted with the observation made in [11] that in the static limit the response of the shell is not very sensitive to changes in the Poisson's ratio. This is clearly not so if the inertia effects are taken into account. It is found then that increasing σ (softer soil) results in very large displacements of the shell wall and, as Figs. 4 and 5 show, in large axial stresses in the shell. For small M the axial stress first decreases with increasing ϵ, but then increases very rapidly with ϵ, the increase being sharper for large σ. It may be noted that for $M \geq 0.1$, N attains asymptotically a constant value for large ϵ, this value being smaller the larger σ is. It is of particular interest to note that if the soil is soft and $M \geq 0.1$, N increases very rapidly with ϵ reaching a maximum value several times larger than 1 and then drops rapidly to an almost constant value that is not much larger than one. In harder soil, however, N does not reach a sharp maximum. Except for small ϵ it steadily increases to a constant value. These observations seem to be consistent with the evidence that pipes suffer greater damage in soft soils.

The variations of W and N with M and ϵ are shown in Figs. 6 and 7 for $\ell = \pi/3$ and $\sigma = 0.25$. It is seen that both W and N behave quite differently as the wavelength is increased. Generally, however, it may be observed that for small M the behavior of W and N with changes in ϵ is the same as for $\ell = \pi/6$, the difference being that the dynamic axial stress is smaller than its statical value for a large range of ϵ. It may be seen that for small ϵ, W first increases sharply when M is small and then drops rapidly, goes through a minimum. The sharp increase for small M and ϵ becomes steeper as ℓ increases (see Figs. 8 and 10). N also behaves in a similar manner.

The variations of W and N with M and ϵ for large ℓ are shown in Figs. 8 - 11. The most important feature to be noticed in these figures is that the pipe begins resonating at a particular frequency that depends on M and ℓ. This has been discussed earlier. Figs. 12 and 13 show the dependence of the resonant behavior when $\sigma = 0.45$. It may be noted that increasing the Poisson's ratio for the same $M (\gtrsim 0.1)$ generally results in larger displacements and axial stresses.

A general behavior that may be observed from these figures is that for small M and ϵ both W and N decrease with increasing σ. However, this behavior is reversed for large M. Also to be observed is the fact that for small M and large ϵ both W and N increase with increasing σ.

In order to see whether the pipe generally follows the motion of the ground for long wavelengths, the values of the radial and axial displacements normalized with respect to the corresponding ground displacements are plotted against ϵ for different M when $\ell = \pi/6$. It may be noted that for very small ϵ only $\overline{U}$ is close to unity if M is large, but $\overline{W}$ is not. It is also interesting to note that for large M, $\overline{W}$ is close to unity when ϵ is large. For small M an increase in the Poisson's ratio is seen to cause smaller discrepancies between the radial and axial displacements of the pipe wall and the corresponding ambient ground displacements.

Thus the following conclusions may be drawn from the above observations.

(1) For long wavelengths when the rigidity ratio of the ground and the pipe is kept at the same small value, larger axial stresses in the pipe are caused in a softer ground. For large rigidity ratios, on the other hand, just the reverse occurs, except when frequency is low.

(2) Pipe resonance occurs only when the rigidity ratio is large and the wavelength is small. No resonance occurs in a soft soil.

(3) For short wavelengths, it appears that the axial stress in the pipe is usually larger in a softer ground except at some small ranges of frequencies.

(4) It is important to note that except for very long wavelengths larger axial stresses are caused in the pipeline in a rocky environment than in a soil-like one.

Acknowledgment

This work was supported in part by the Problem Focused Research Division of the National Science Foundation (Grant No. PFR-7822848) under the Earthquake Hazards Mitigation Program. The program manager was Dr. W.W. Hakala. Part of this work was done while the first author (SKD) was at the Department of Applied Mathematics, Calcutta University. He is grateful to Professor P.K. Ghosh for his support and help. Thanks are also due to Natural Science and Engineering Science Council of Canada for providing partial support to AHS.

References

1. Wang, L.R.L. and O'Rourke, M., "State of the Art of Buried Lifeline Earthquake Engineering," Proceedings of the Current State of Lifeline Earthquake Engineering, ASCE, Los Angeles, Calif., August 30-31, 1977, pp. 252-266.

2. Ariman, T. and Muleski, G.E., "Recent Developments in Seismic Analysis of Buried Pipelines," Proceedings of the 2nd U.S. National Conference on Earthquake Engineering, Earthquake Engineering Research Institute, Berkeley, Calif., August 22-24, 1979, pp. 643-652.

3. Nelson, I. and Weidlinger, P., "Dynamic Seismic Analysis of Long Segmented Lifelines," Journal of Pressure Vessel Technology, Trans. ASME, Vol. 101, 1979, pp. 10-20.

4. Kubo, K., Katayama, T., and Ohashi, M., "Lifeline Earthquake Engineering in Japan," Journal of the Technical Councils of ASCE, TC1, April 1979, pp. 221-238.

5. Muleski, G.E., Ariman, T., and Aumen, C.E., "A Shell Model of a Buried Pipe in a Seismic Environment," Journal of Pressure Vessel Technology, Trans. ASME, Vol. 101, 1979, pp. 44-50.

6. Novak, M. and Hindy, A., "Dynamic Response of Buried Pipelines," Proceedings of the Sixth European Conference on Earthquake Engineering, Dubrovnik, Yugoslavia, September 1978, Vol. 2, pp. 533-540.

7. Hindy, A. and Novak, M., "Earthquake Response of Underground Pipelines," International Journal of Earthquake Engineering and Structural Dynamics, Vol. 7, 1979, pp. 451-476.

8. Novak, M. and Hindy, A., "Seismic Analysis of Underground Tubular Structures," Seventh World Conference on Earthquake Engineering, September 8-13, 1980.

9. El-Akily, N. and Datta, S.K., "Response of a Circular Cylindrical Shell to Disturbances in a Half-Space," To appear in the International Journal of Earthquake Engineering and Structural Dynamics, 1980.

10. N. El-Akily and Datta, S.K., "Response of a Buried Pipe to Seismic Waves," Seventh World Conference on Earthquake Engineering, September 8-13, 1980.

11. Datta, S.K. and El-Akily, N., "Seismic Response of a Buried Pipe in an Infinite Medium," To be published. Also available as CUMER Report 80-3, June 1980, Department of Mechanical Engineering, University of Colorado, Boulder, Colorado.

12. Bleich, H.H. and Baron, M.L., "Free and Forced Vibrations of an Infinitely Long Cylindrical Shell in an Infinite Acoustic Medium," Journal of Applied Mechanics, Transactions of ASME, Vol. 21, 1954, pp. 167-177.

13. Junger, M.C., "Dynamic Behavior of Reinforced Cylindrical Shells in a Vacuum and in a Fluid," Journal of Applied Mechanics, Transactions of ASME, Vol. 21, 1954, pp. 35-41.

Table 1

Real Vibrational Frequencies ($\epsilon = \omega R/C_{\ell}$) of the Shell in an Elastic Medium

($m = 0.05$, $\nu = 0.3$, $\sigma = 0.25$, $\rho^* = 2.9266$)

ℓ	$M = \mu/G$			
	0.10	0.30	1.0	10
0 0.523599 1.047198	None	None	None	None
1.570796	None	None	None	0.90349
2.094395	None	None	1.186374	1.156917
2.617994	None	1.503563	1.441541	1.386536
3.141593	None	1.778986	1.686290	1.598974
3.665191	None	2.045781	1.923659	1.795699
4.188700	None	2.306060	2.155022	1.976985
4.712389	None	2.560788	2.381172	2.142921
5.235988	2.995772	2.810588	2.602665	2.293865
5.759587	3.266147	3.055966	2.819936	2.430641
6.283185	3.530997	3.297378	3.033356	2.554559 3.571390

Table 2

Real Vibrational Frequencies ($\epsilon = \omega R/C_1$) of the Shell in an Elastic Medium

($m = 0.05$, $\nu = 0.3$, $\sigma = 0.45$, $\rho^* = 2.9266$)

ℓ	$M = \mu/G$			
	0.10	0.30	1.0	10
0 0.523599 1.047197	None	None	None	None
3.141592	None	0.9339887	0.8997447	0.8699774
6.283185	1.845795	1.741516	1.646022	1.444238 1.865283

List of Figures

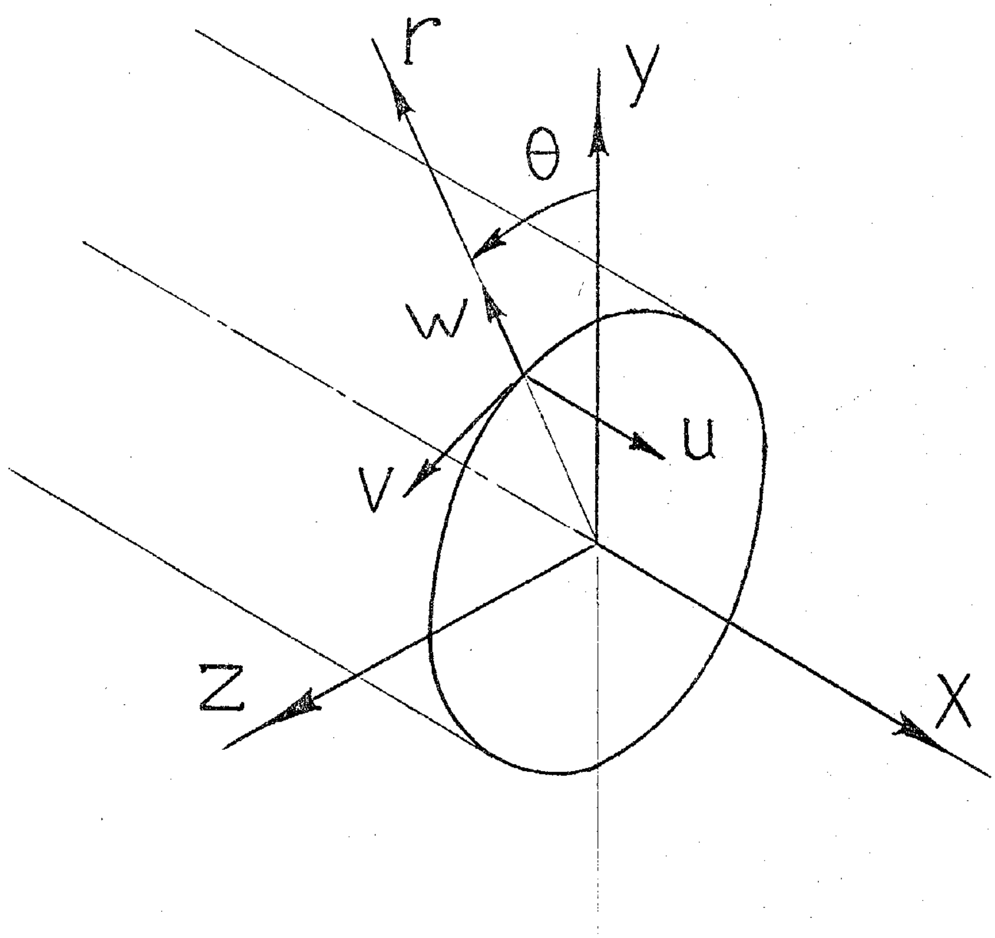

Figure 1. Geometry of the Problem

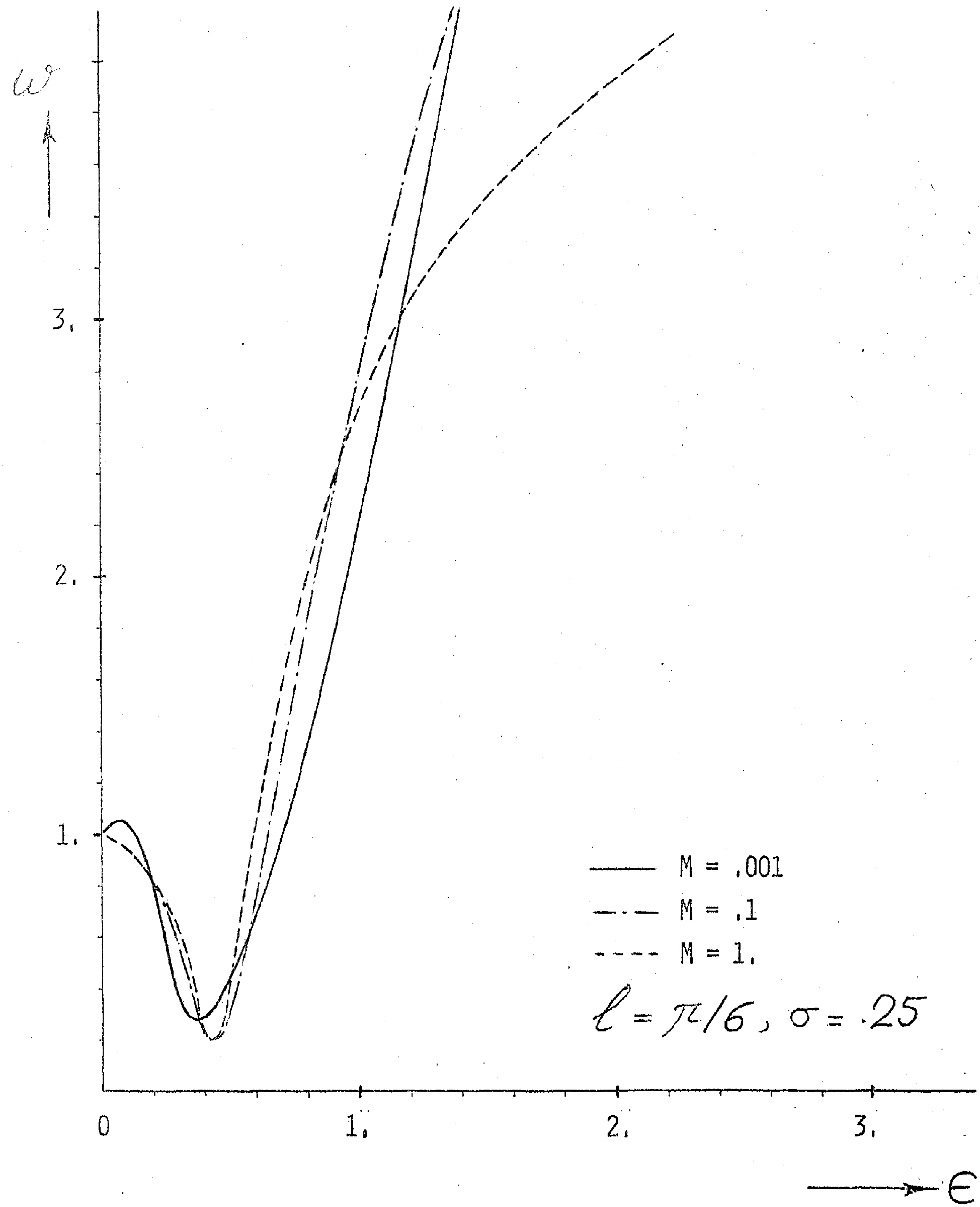

Figure 2. Variation of w with ε for different M at long wavelengths (σ = 0.25)

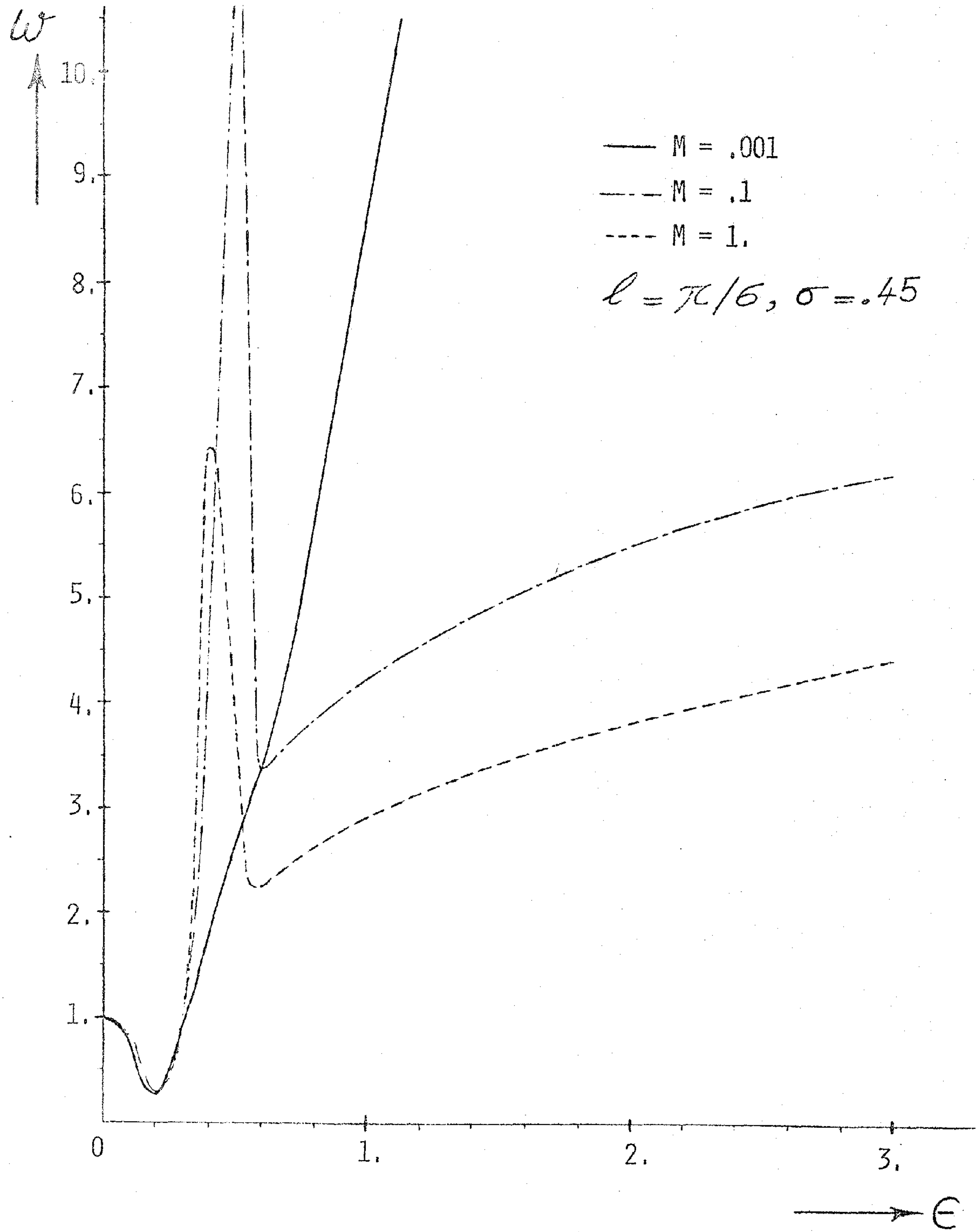

Figure 3. Variation of w with ε for different M at long wavelengths (σ = 0.45)

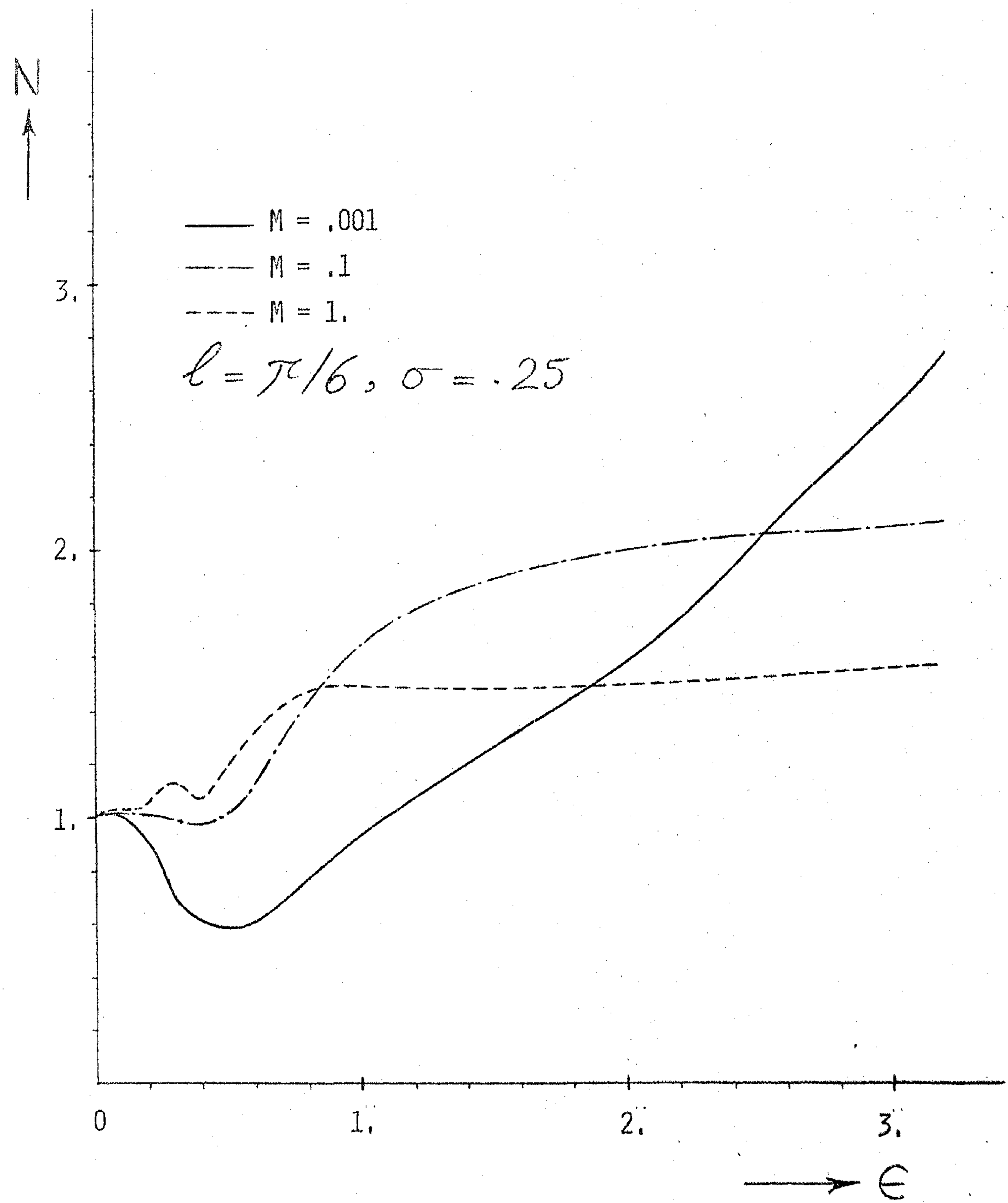

Figure 4. Axial stress variation with ϵ for different M at long wavelengths (σ = 0.25)

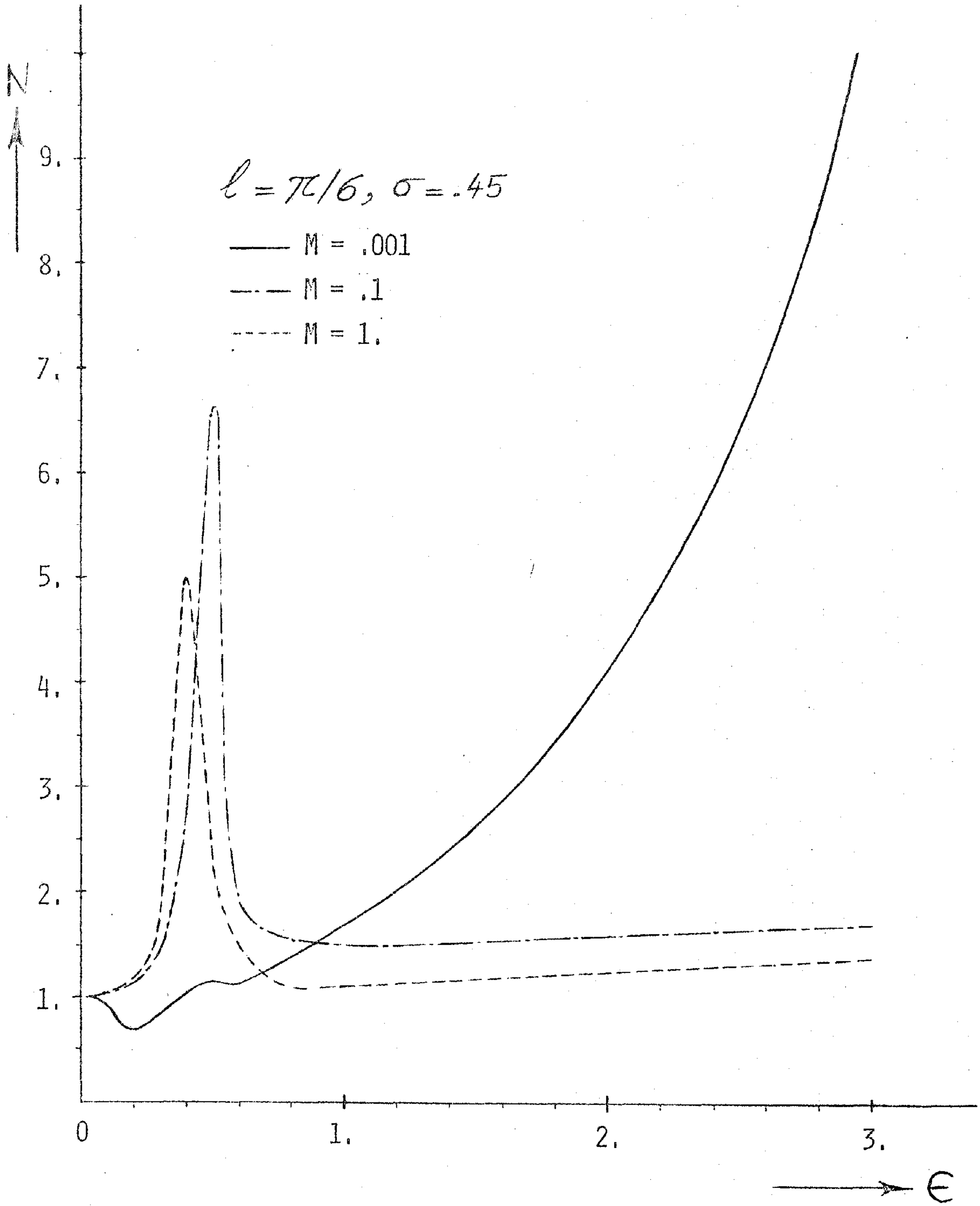

Figure 5. Axial stress variation with ε for different M at long wavelengths (σ = 0.45)

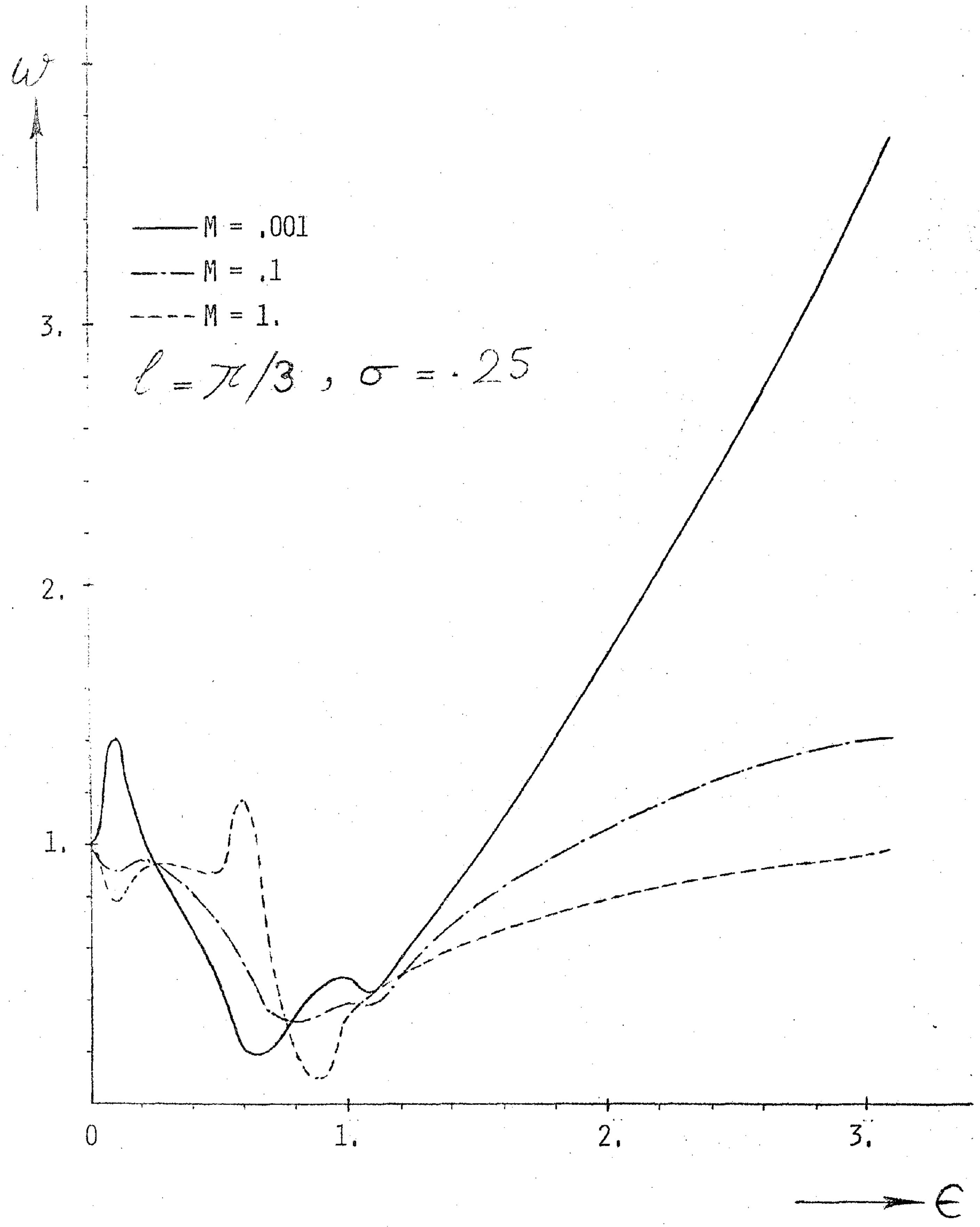

Figure 6. Radial displacement of the shell for different M

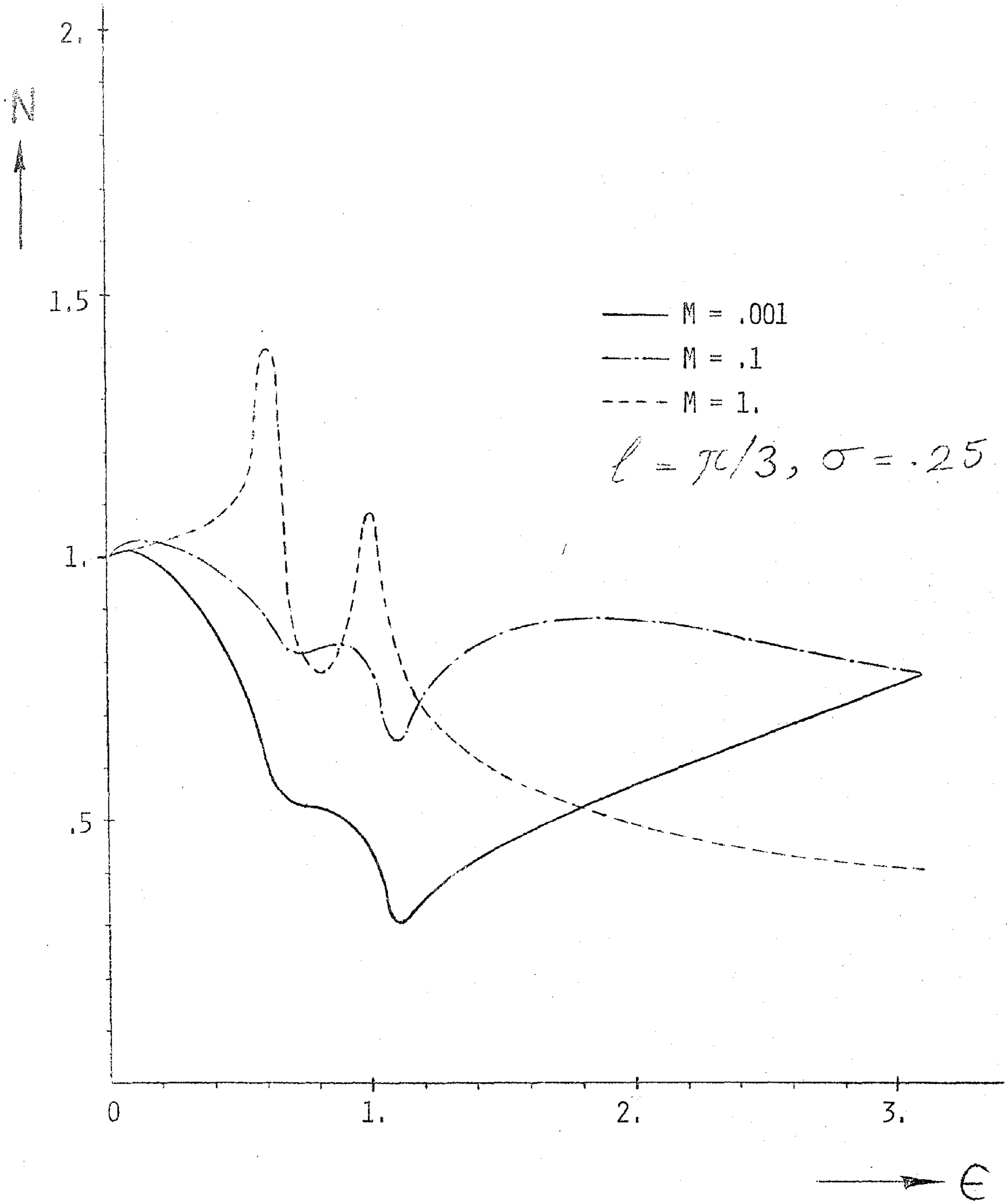

Figure 7. Axial stress in the shell for different M

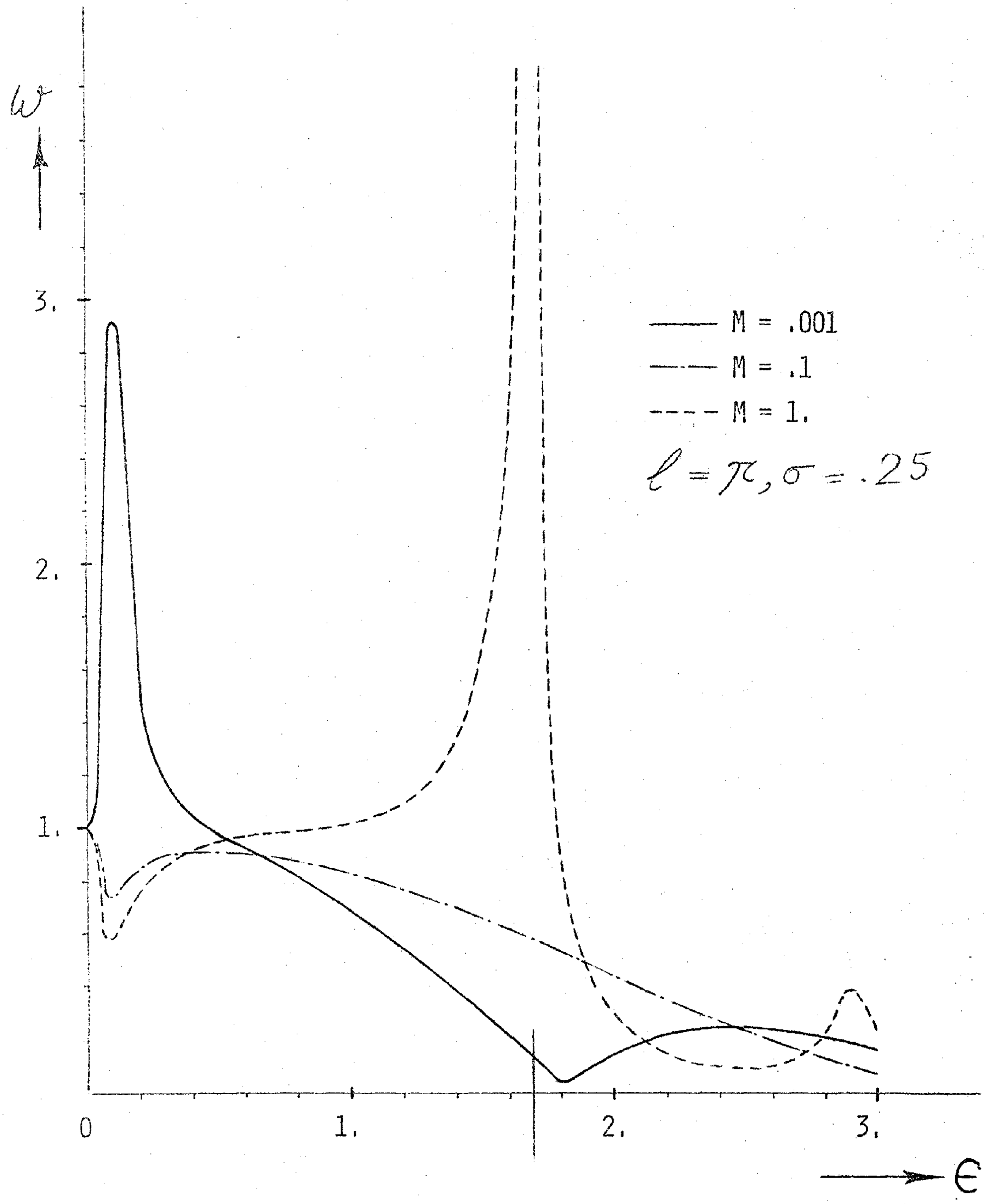

Figure 8. Radial displacement of the shell at short wavelengths

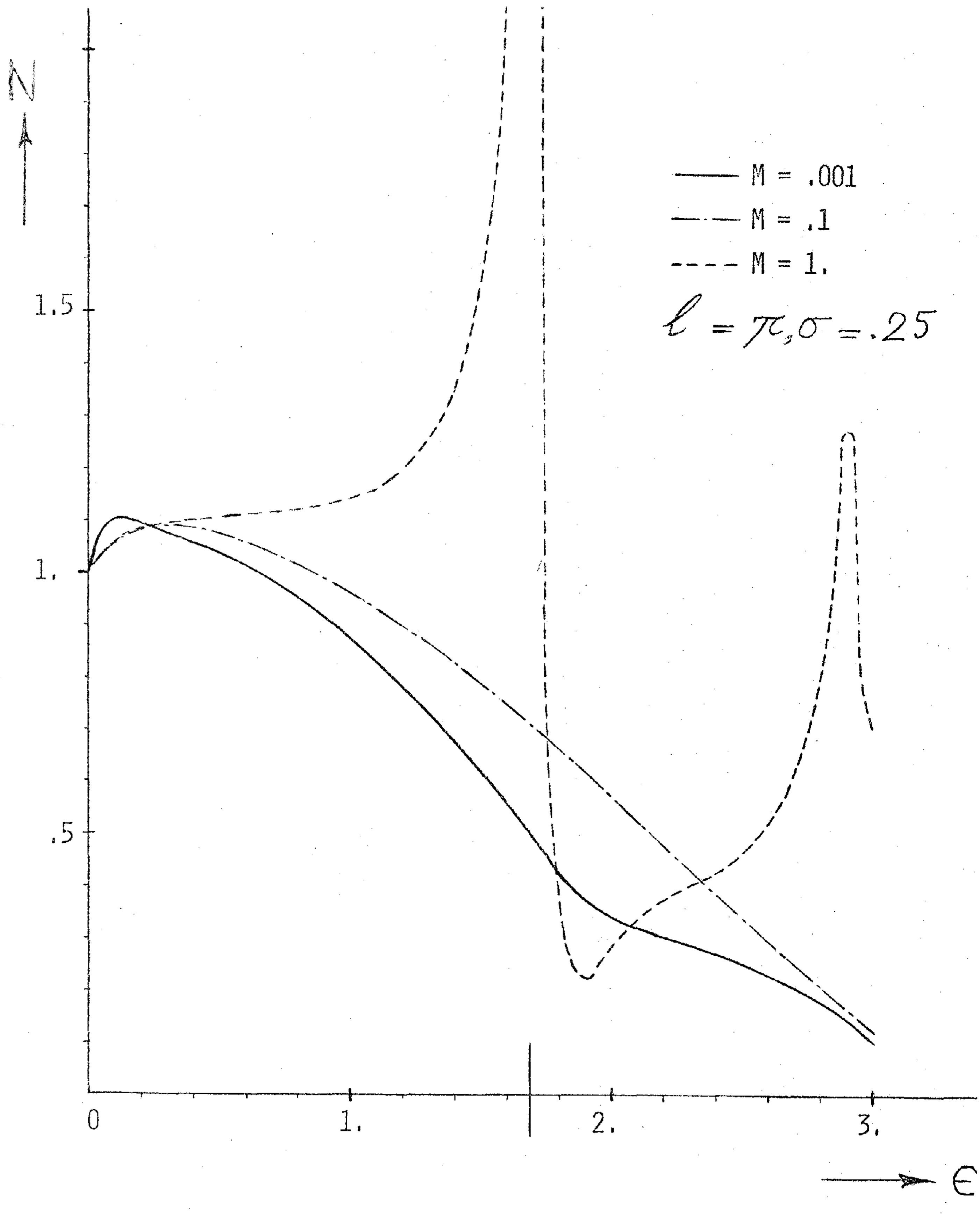

Figure 9. Axial stress in the shell at short wavelengths

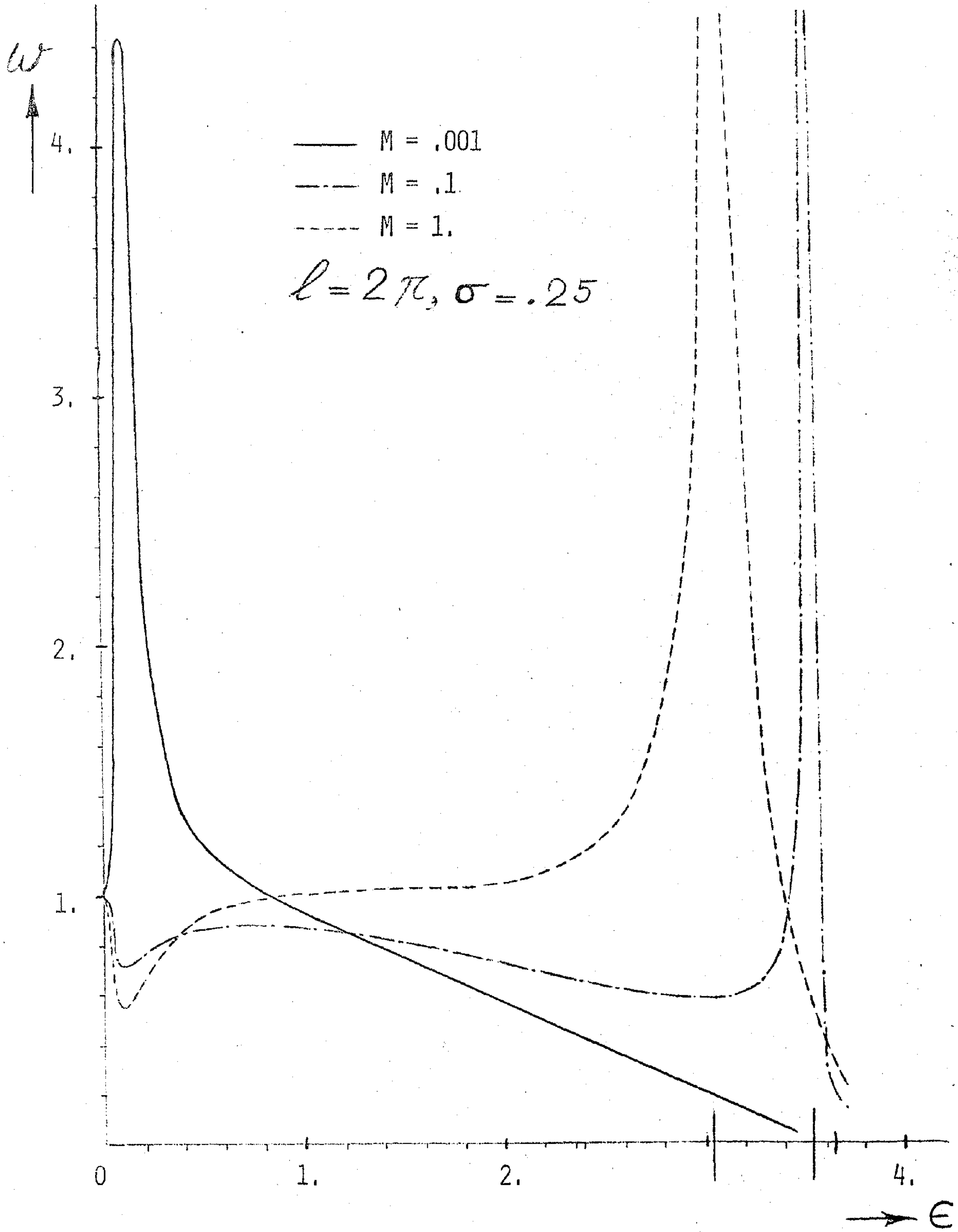

Figure 10. Radial displacement of the shell at short wavelengths ($\sigma = 0.25$)

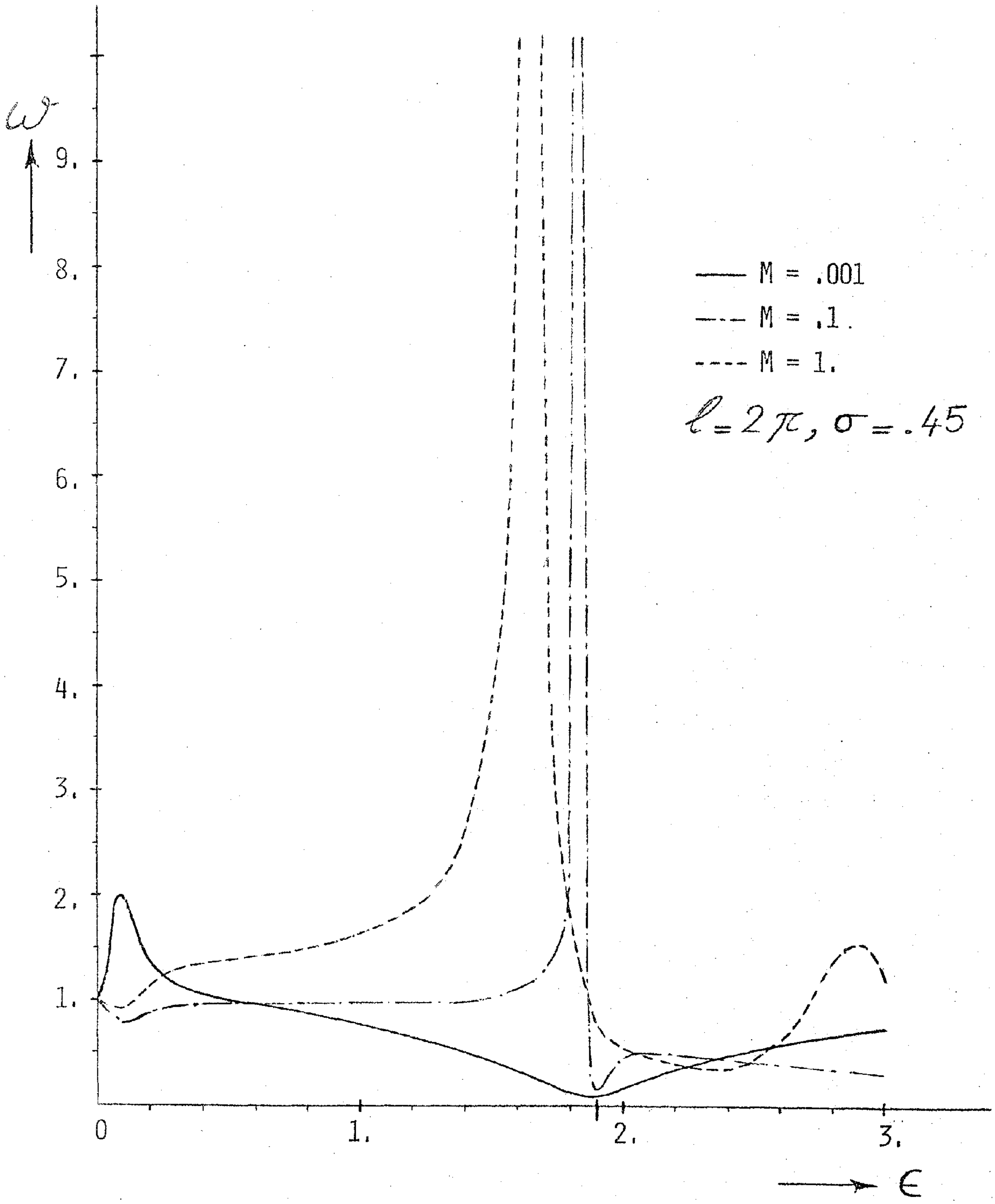

Figure 11. Radial displacement of the shell at short wavelengths (σ = 0.45)

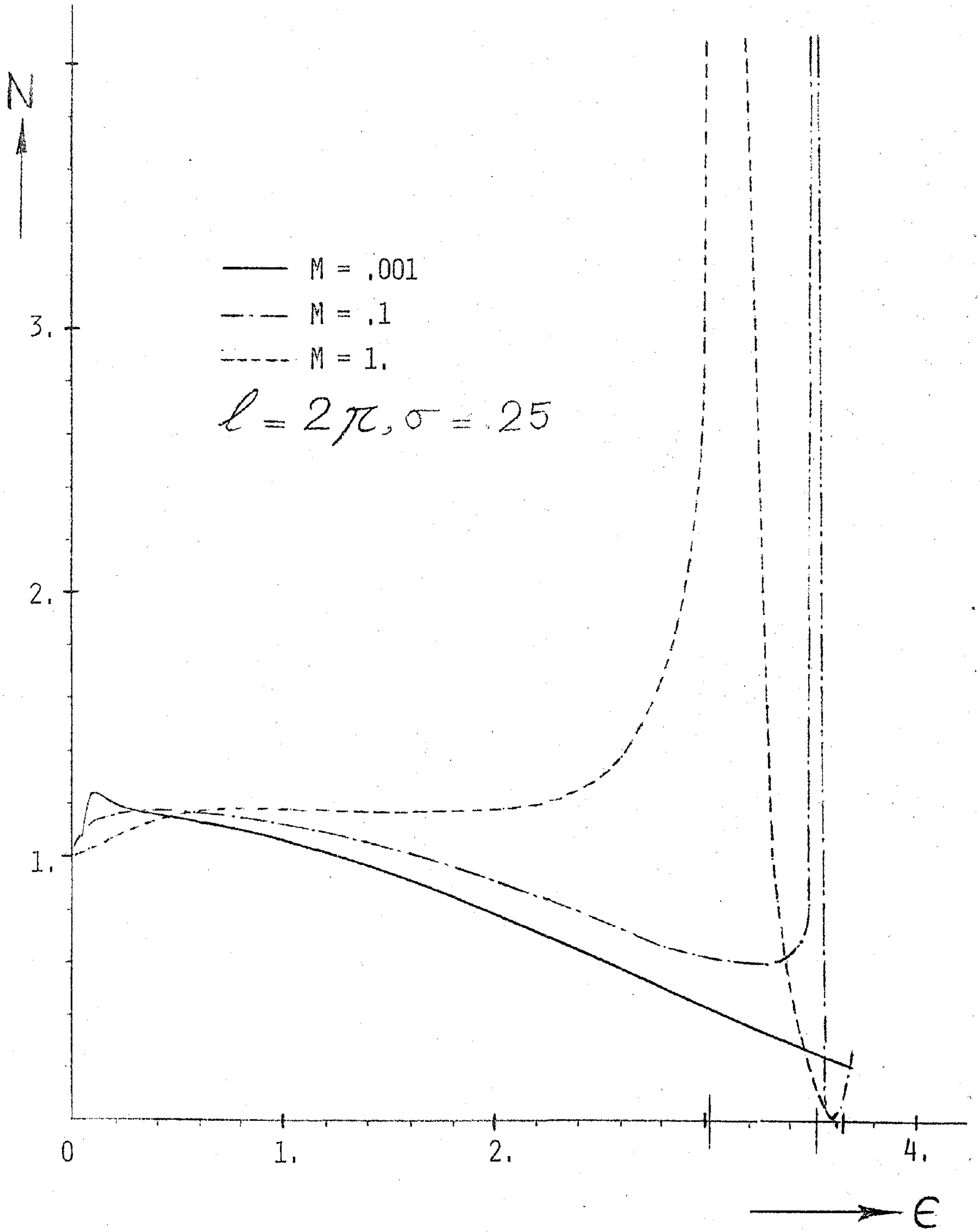

Figure 12. Axial stress in the shell at short wavelengths (σ = 0.25)

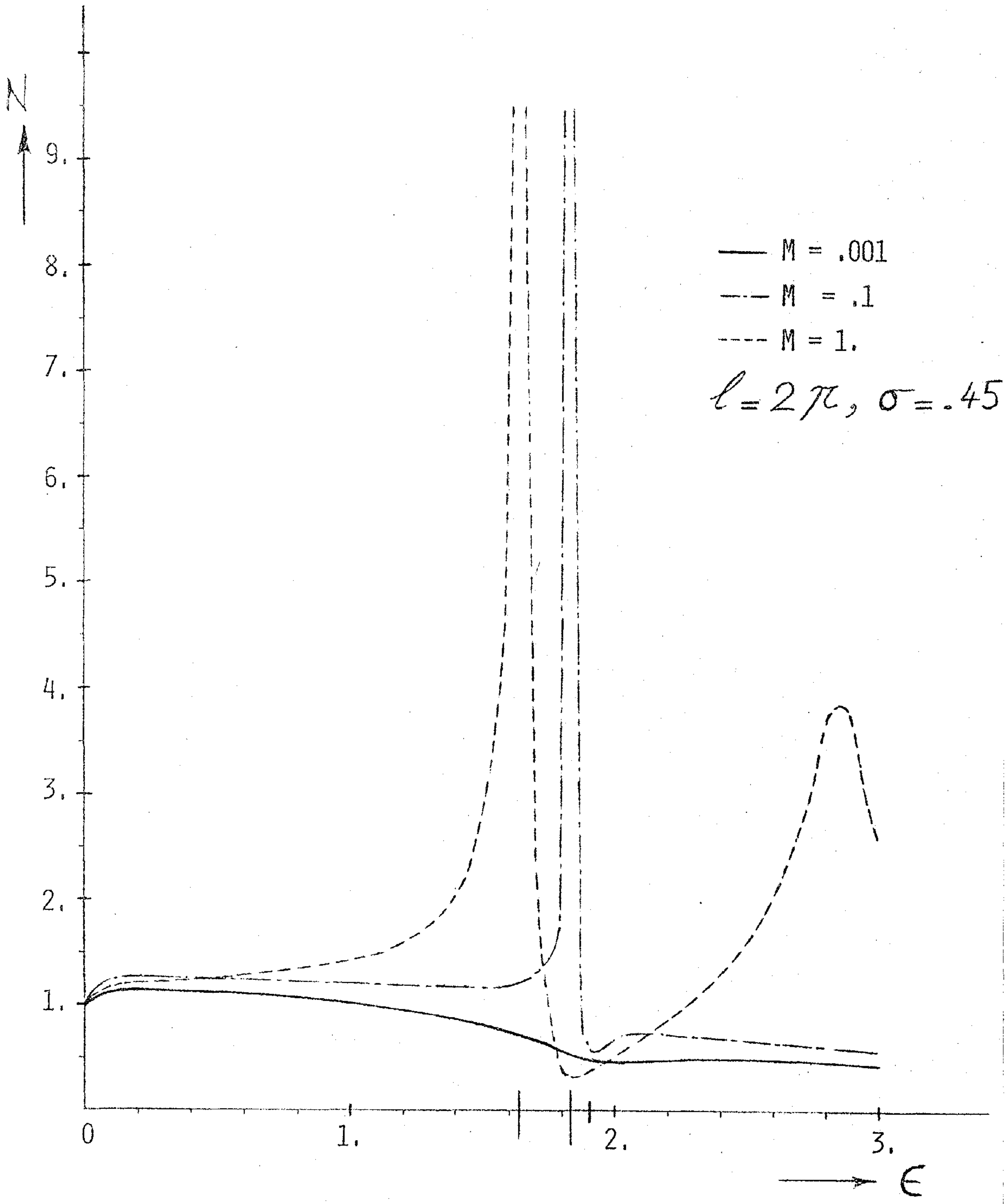

Figure 13. Axial stress in the shell at short wavelengths (σ = 0.45)

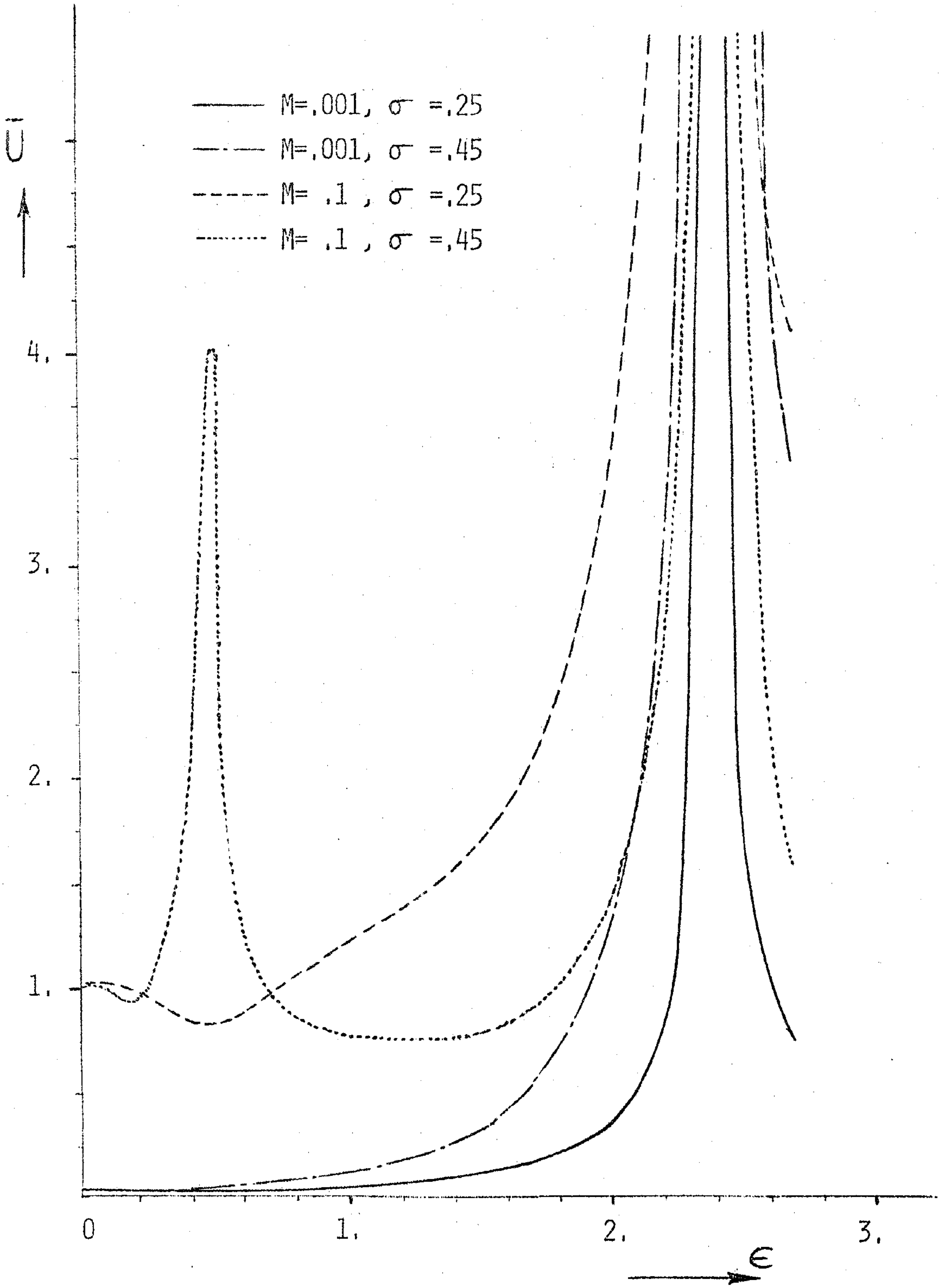

Figure 14. Axial displacement of the shell relative to the incident axial displacement

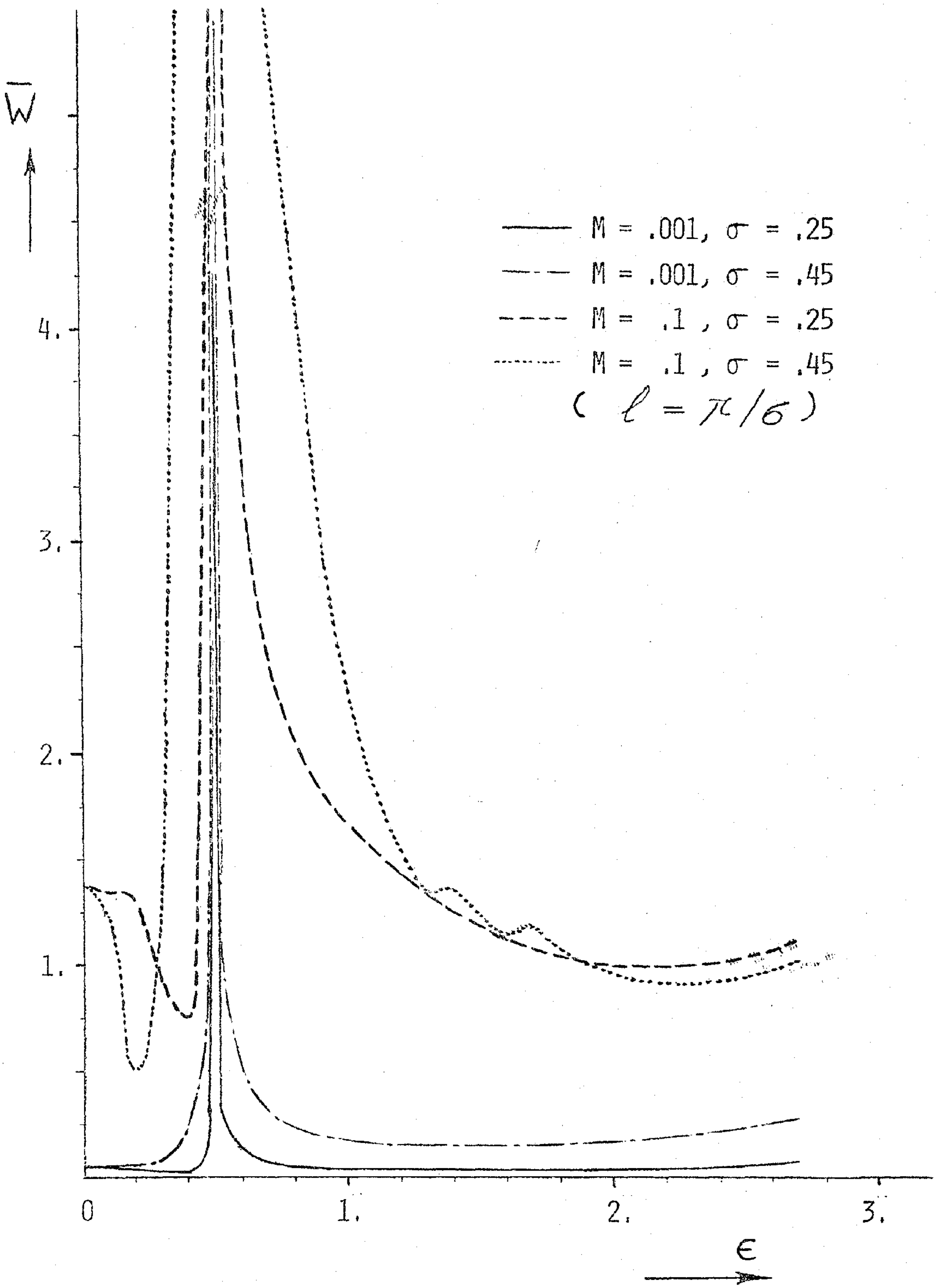

Figure 15. Radial displacement of the shell relative to the incident radial displacement

REPORT DOCUMENTATION PAGE	1. REPORT NO. NSF/RA-800214	2.	3. Recipient's Accession No. PB81 119513

4. Title and Subtitle Dynamic Response of a Buried Pipe in a Seismic Environment	5. Report Date August 1980
	6.
7. Author(s) S. K. Datta, A. H. Shah, N. El-Akily	8. Performing Organization Rept. No. CUMER-80-5
9. Performing Organization Name and Address University of Colorado Department of Mechanical Engineering Boulder, CO 80309	10. Project/Task/Work Unit No. 11. Contract(C) or Grant(G) No. (C) (G) PFR7822848
12. Sponsoring Organization Name and Address Engineering and Applied Science (EAS) National Science Foundation 1800 G Street, N.W. Washington, D.C. 20550	13. Type of Report & Period Covered 14.

15. Supplementary Notes

16. Abstract (Limit: 200 words)

Axisymmetric dynamic response of a buried pipe due to an incident compressional wave is the subject of this study. The pipe has been modelled as a thin cylindrical shell of linear homogeneous isotropic elastic material embedded in a linear isotropic homogeneous elastic medium of infinite extent. The response characteristics of the pipe due to changes in the material properties of the surrounding medium have been studied. It was found that even at long wavelengths and low frequencies the dynamic response is significantly altered by the changes in the Poisson's ratio and the rigidity modulus of the surrounding medium. In addition, it was found that there are real resonant frequencies of the pipe which are also significantly dependent on these quantities as well as on the wavelength.

17. Document Analysis a. Descriptors

Dynamic response	Pipelines
Seismic waves	Cylindrical shells
Earth movements	Earthquakes

b. Identifiers/Open-Ended Terms

Earthquake Hazards Mitigation

c. COSATI Field/Group

18. Availability Statement	19. Security Class (This Report)	21. No. of Pages
NTIS	20. Security Class (This Page)	22. Price

(See ANSI–Z39.18) See Instructions on Reverse

OPTIONAL FORM 272 (4–77)
(Formerly NTIS–35)
Department of Commerce